Multiple Single Cell Screening and DNA MDA Amplification Chip for Oncogenic Mutation Profiling

Ren Li[1,2,5], Mingxing Zhou[1] , Chunyan Yue[1], Weikai Zhang[1], Yan Ma[1], Hailin Peng[2], Zhiyuan Hu[1,3,4,5]*, Zewen Wei[1]*

1 CAS Key Laboratory of Standardization and Measurement for Nanotechnology, CAS Center for Excellence in Nanoscience, National Center for Nanoscience and Technology of China, Beijing 100190, China.

2 Academy for Advanced Interdisciplinary Studies, Peking University, Beijing 100871, China

3 Sino-Danish College, University of Chinese Academy of Sciences, Beijing 100049, P. R. China

4 Center for Neuroscience Research, School of Basic Medical Sciences, Fujian Medical University, Fuzhou, Fujian Province, China.

5 University of Chinese Academy of Sciences, Beijing 100049, P. R. China

* Authors for correspondence, Zhiyuan Hu (Huzy@nanoctr.cn, Fax 86-10-82545643) or Zewen Wei (weizw@nanoctr.cn, Fax 86-10-82545752).

Supplementary Figure S1

Using the membrane of tri-states valves as an active mixer

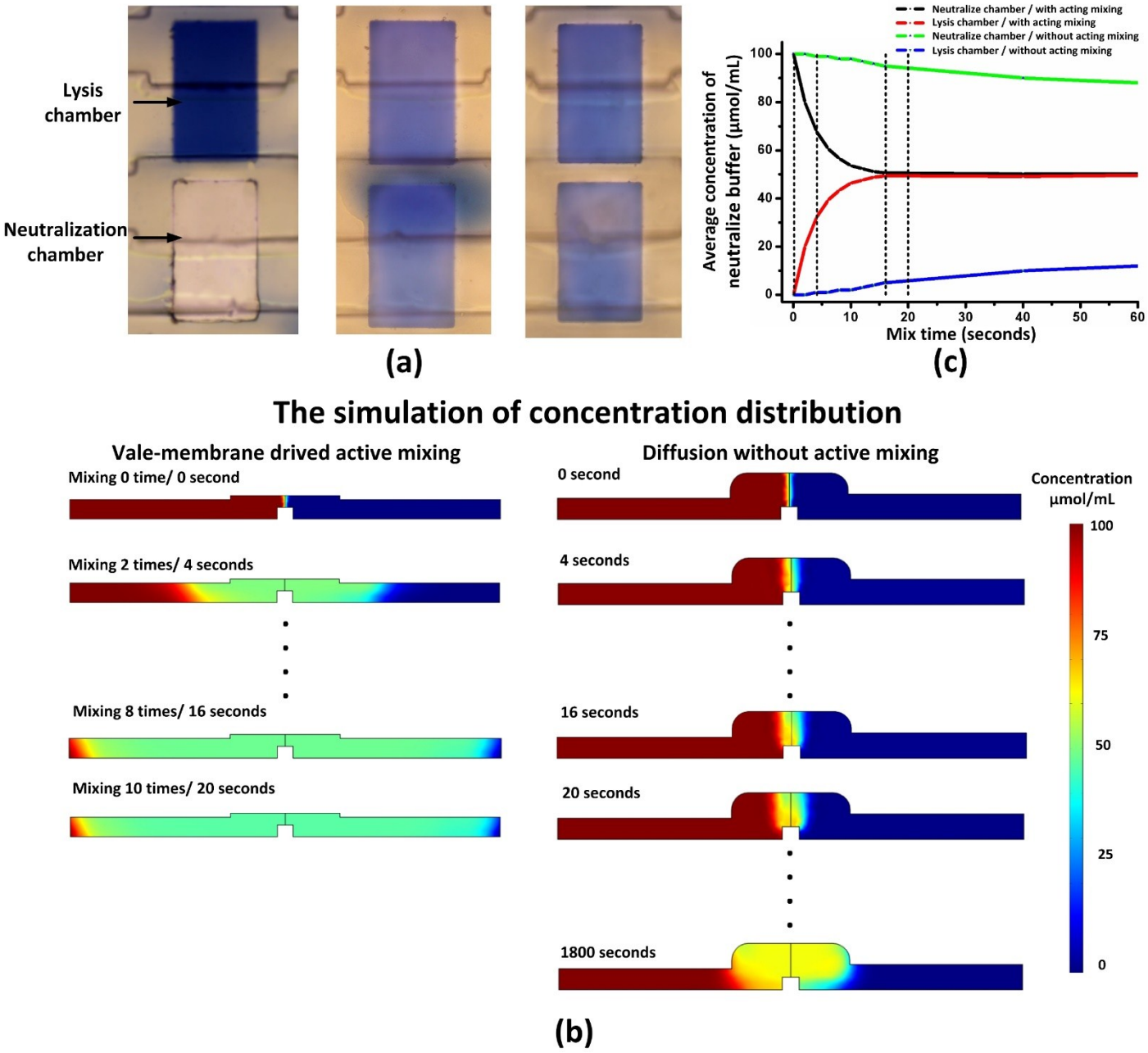

To mix different liquids in neighboring chambers (illustrated in left image of figure (a) as blue color and transparent), the membrane of tri-states valve was repetitively switched open (as shown in middle image of figure (a), in which the valve area was filled by blue liquids) and close for 10 times, till reagents were homogeneously mixed (right image of figure (a)). Using a FEA (Finite Element Analysis) software COMSOL Ver5.0, the membrane driven active mixing process was 2-D simulated (left images of figure (b)). The dimensional parameters were set according to the real microfluidic chip. The initial concentrations of liquid in lysis (left) and neutralization (right) chambers were set at 100 and 0 μmol/mL. Each cycle of valve open/close costs 2 seconds. For comparison, a natural diffusion process was also simulated with the same parameters (right images of figure (b)). To ensure maximum diffusion, the valve was maintained full-open in the simulation regarding natural diffusion. Figure (b) shows the quantitative data of the variation of mean liquid concentrations in lysis and neutralization chambers. From left to right, dashed lines indicate time points of 0, 4, 16 and 20 seconds. The simulations demonstrate that 8~10 times of active mixing (taking 16 ~ 20 seconds) result in homogeneous mixing, while mixing is far more insufficient under the natural diffusion

mode. Moreover, prolonging the mixing time of natural diffusion to 1800 seconds barely improves the mixing status.

Supplementary Figure S2

The computer assisted microfluidic chip operating system

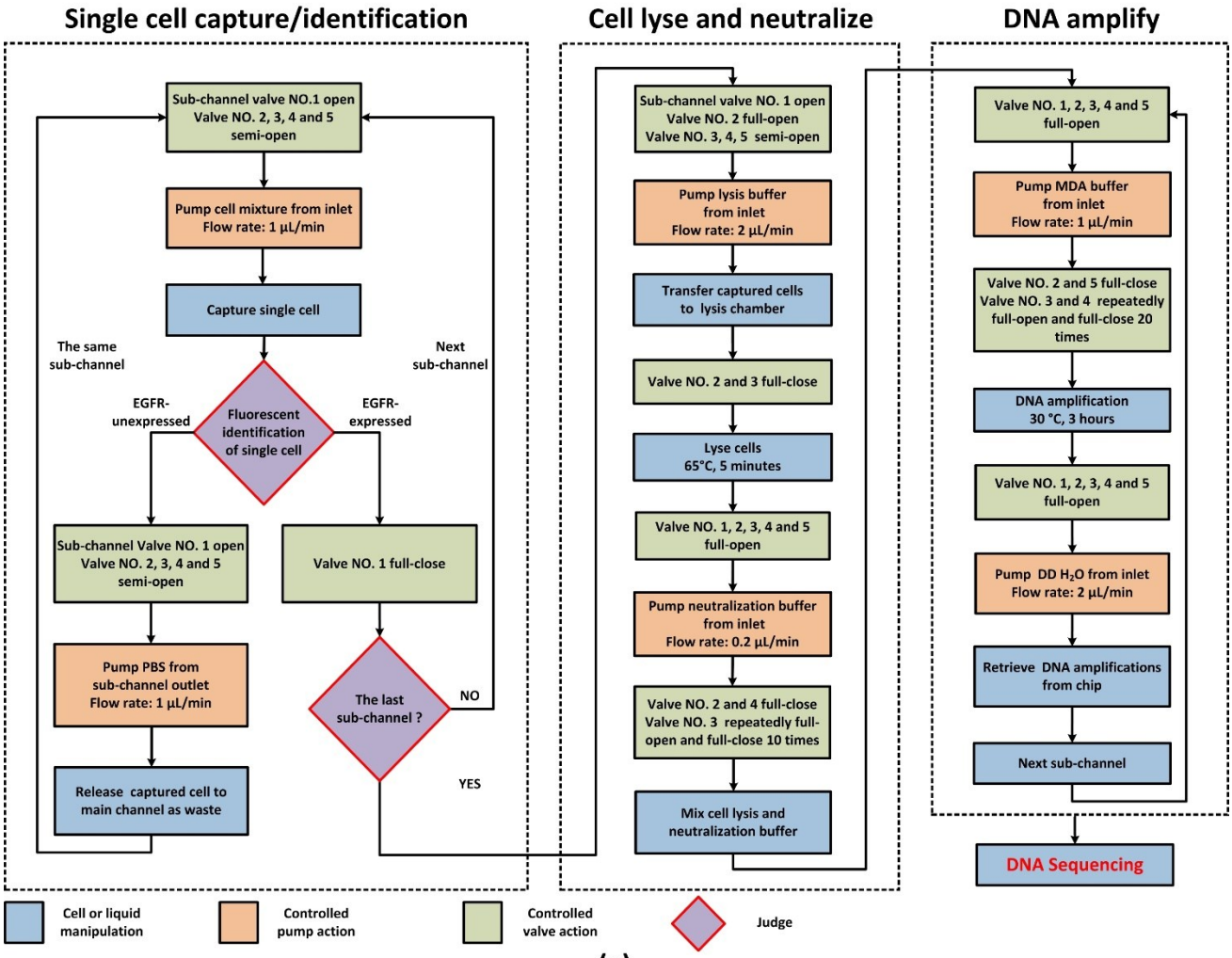

(a)

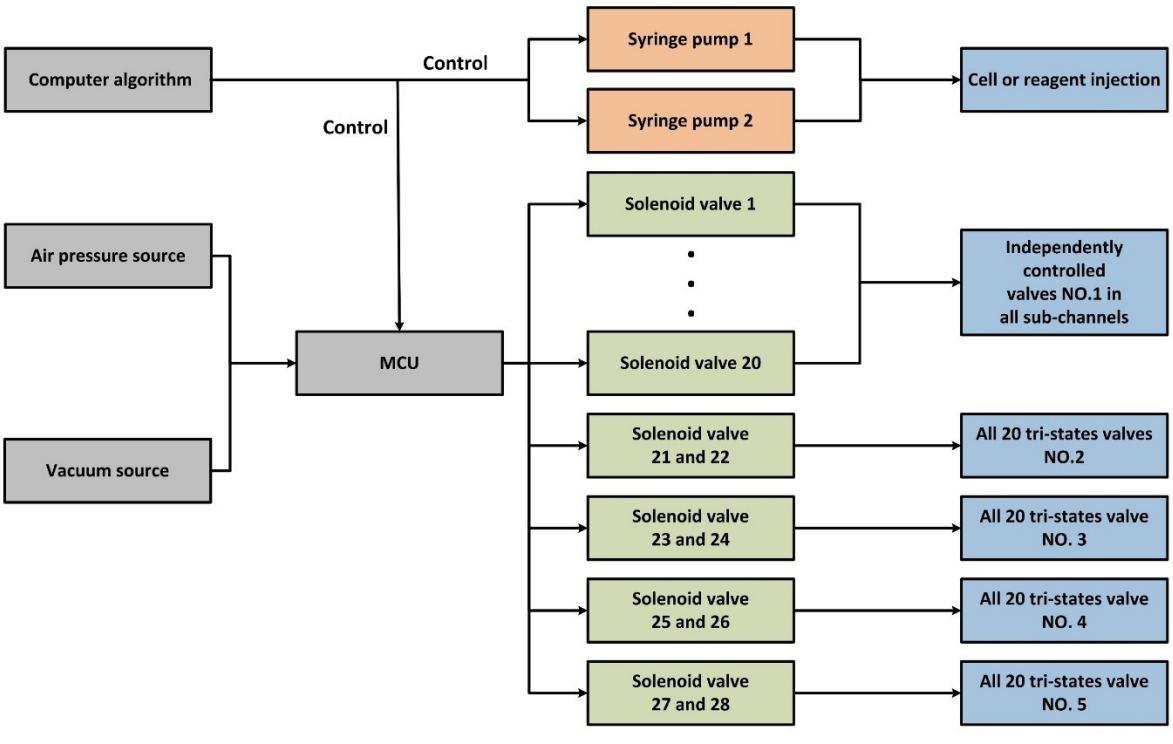

(b)

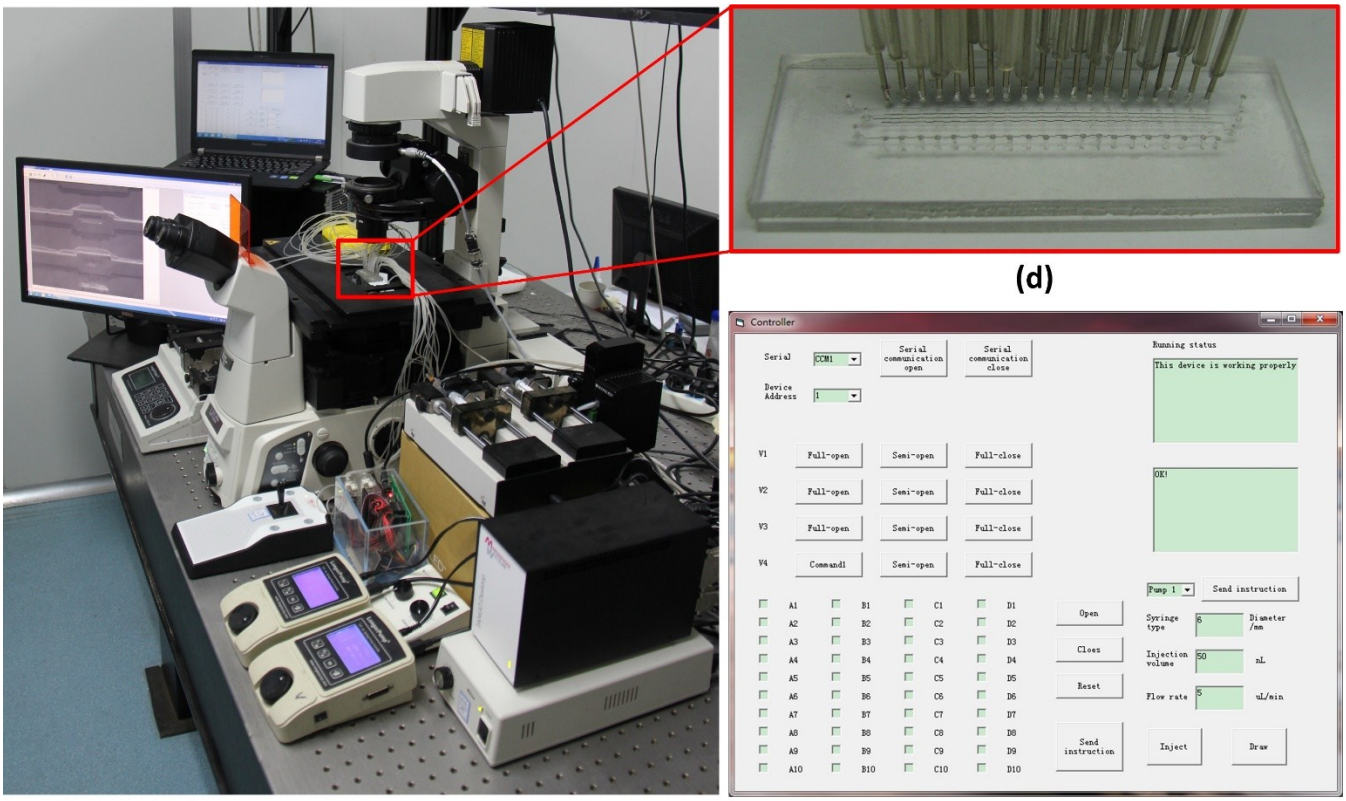

Figure (a) illustrates logical flowchart of the controlling algorithm which consists of 3 main parts. Single cell capture/identification was sequentially performed in 20 sub-channels, while cell lysis, neutralize and DNA amplification were performed in parallel. Figure (b) demonstrates the connection diagram of different off-chip controlling devices. Two syringe pumps, which were used to inject cell mixtures or reagents, were directly controlled by computer. An Intel 8051 MCU (Microcontroller Unit), which was controlled by computer, was used to switching the connection between air pressure / vacuum source and 28 solenoid valves. Hence, all on-chip valves were controlled by computer. Figure (c) is the photo of the system setup, which includes a Nikon fluorescent microscopy with CCD, a controlling computer, two syringe pumps, 28 solenoid valves and MCU. Figure (d) is the photo of the microfluidic chip in which only 20 valves No. 1 were connected for demonstration. Figure (e) shows the interface of the compiled algorithm running on Windows system.

Supplementary Figure S3

The assessment of MDA DNA amplification product.

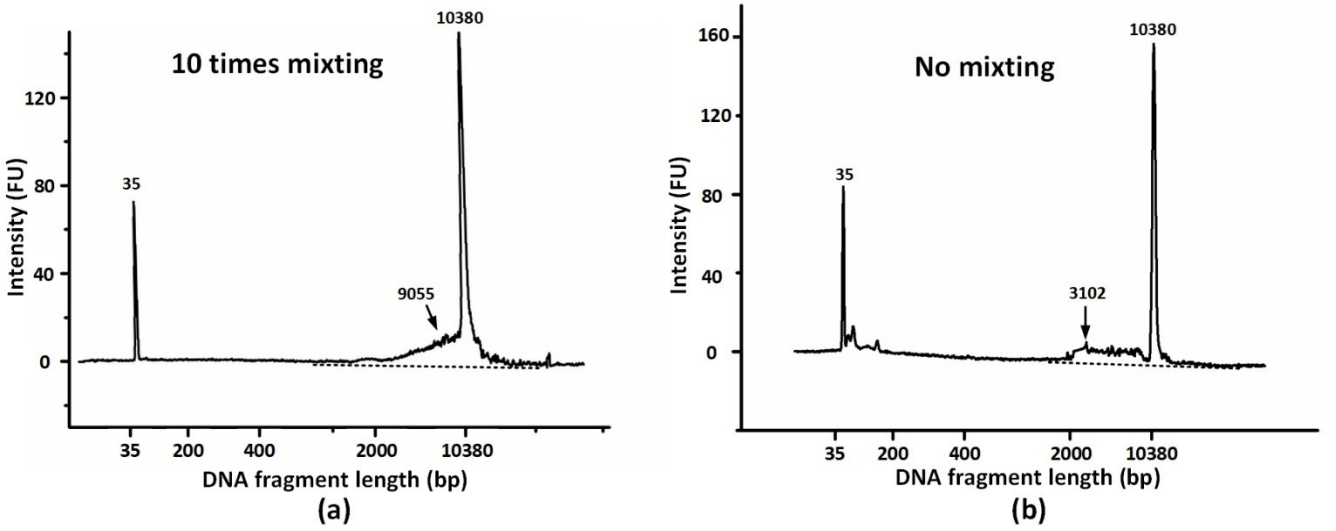

The MDA (Multiple Displacement Amplification) amplification products of single A549 cells, were examined using Agilent 2100 Electrophoresis Bioanalyzer (Agilent, USA). (a) The reagents were mixed 10 times on chip with the assistance of tri-state valves. The main peak of fragment length locates in 9,055 bp, matching the typical value of MDA amplification, which should be around 10,000 bp[1]. Moreover, the total DNA mass and concentration also satisfy the requirements of further PCR amplification and Sanger' sequencing. (b) The reagents were without mixing. The main peak of DNA fragment length was gradually reduced (3,102 bp). The total DNA mass and concentration also decreased.

Supplementary Figure S4

The electropherograms of Sanger's gene sequencing (EGFR)

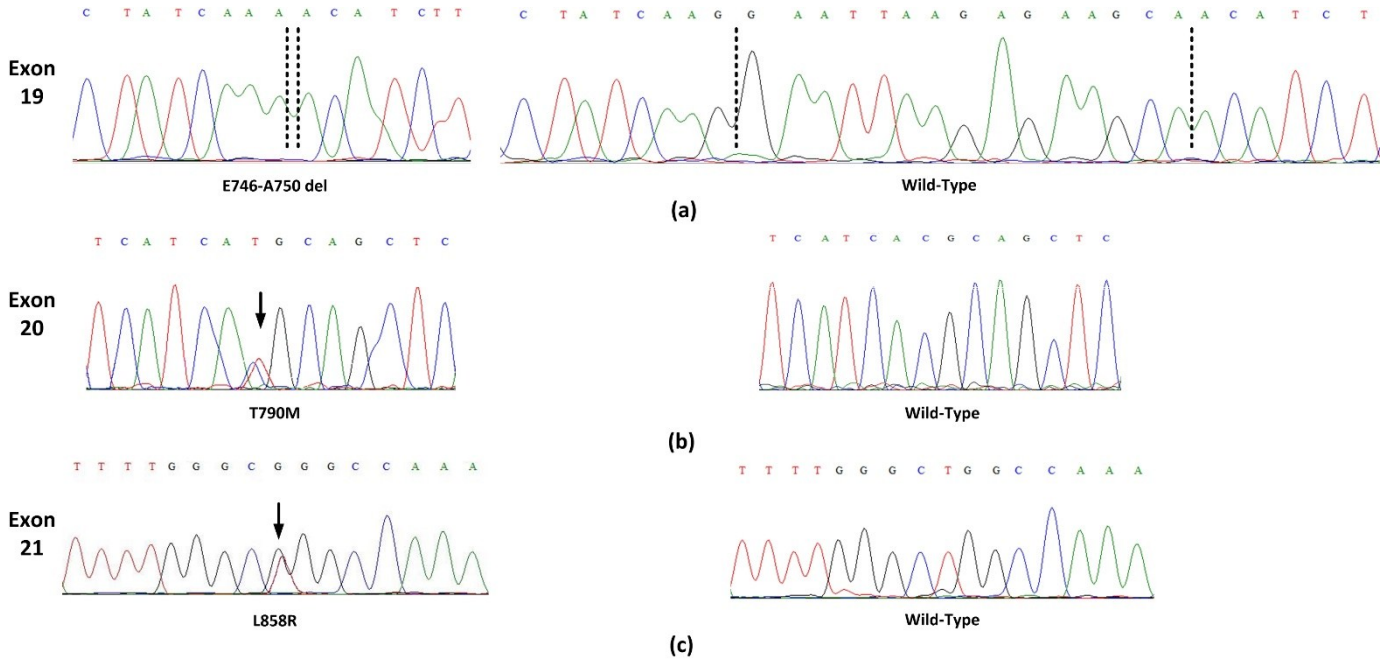

The Supplementary Figure S4 shows the electropherograms of Sanger's gene s*e*quencing in exon 19, 20 and 21 of HCI-1650 single cells. (a) The electropherograms of del E746-A750 mutation and wild type in exon 19. (b) The electropherograms of T790M mutation and wild type in exon 20. (c) The electropherograms of L858R mutation and wild type in exon 21. The arrows point mutation bases, and dashed lines show deletion bases. The wild-type indicates the homozygote which T790M and L858R mutation indicates the heterozygote

Supplementary Figure S5

The electropherograms of Sanger's gene sequencing (TP 53)

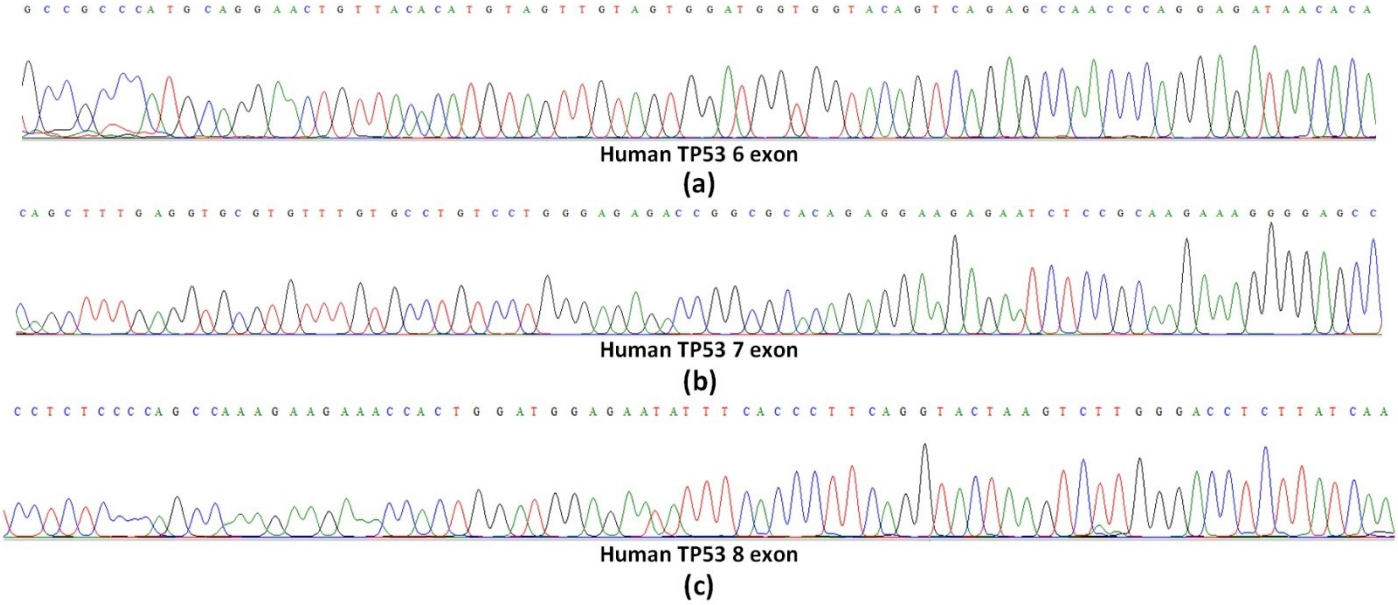

The Supplementary Figure S5 shows the electropherograms of Sanger's gene sequencing in TP53 exon 6, 7 and 8 of a single cell. These exons are reported to have combined effect with EGFR mutation on TKI therapeutic effect[2] . We employed the similar protocol with EGFR assay, the only difference was replacing PCR primers by:

Human TP53 exon 6 forward: 5'- TCTCCCCAAGGCG -3'

Human TP53 exon 6 reverse: 5'- TGGCAAGTGGCTCC -3'

Human TP53 exon 7 forward: 5'- TCTCCCCAAGGCG -3'

Human TP53 exon 7 reverse: 5'- GCTTCTTGTCCTGCTTG -3'

Human TP53 exon 8 forward: 5'- TGCCTCAGATTCACTTTTA -3'

Human TP53 exon 8 reverse: 5'- CACTTGATAAGAGGTCCCA -3'

(a) The electropherograms of wild type in TP53 exon 6. (b) The electropherograms of wild type in TP53 exon 7. (c) The electropherograms of wild type in TP53 exon 8.

Supplementary Figure S6

Sequencing cells from mouse lung

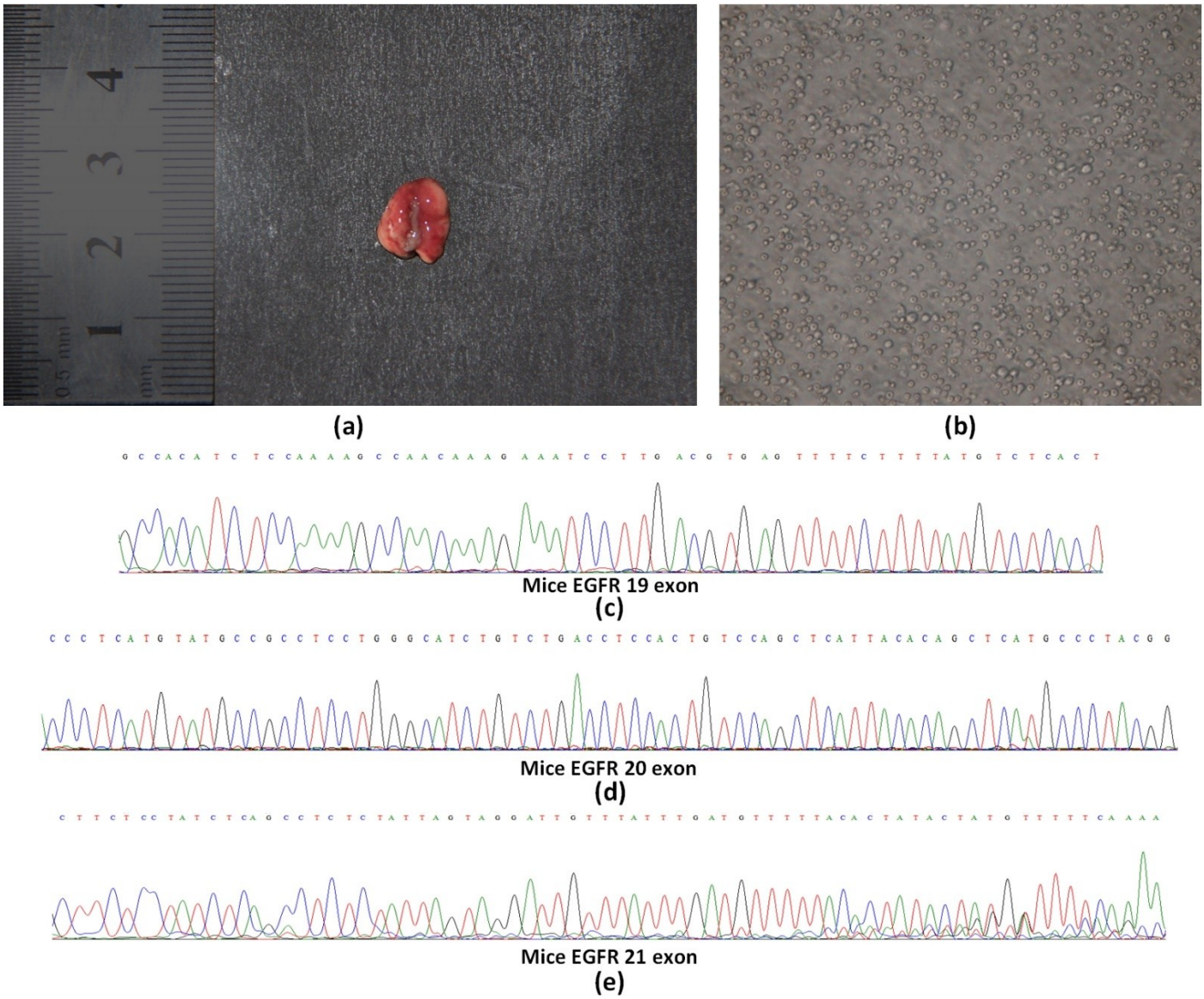

Male C57BL/6 mice (age 6~8 weeks) were dissected and lung tissues (Figure a) were obtained and washed 5 times with PBS. Then lung tissues were washed 3 times by cleaning buffer from a single cell lysis kit (KeyGEN). Each washed lung tissue was cut into pieces and immersed in 1 mL lysis buffer (2 mg/mL) from the same single cell lysis kit at 37 °C for 3 hours. After that, 2 mL rinsing buffer from the same single cell lysis kit was added into each lysate, the mixture was centrifuged (2000 RPM) and the supernatant was removed. The rinsing was repeated 3 times. The cells from rinsed lysate (Figure b) were retrieved and stained by DAPI. 20 single cells were randomly selected and processed by microfluidic chip before being PCR amplified and sequenced respectively.

PCR primers:

Mice EGFR exon 19 forward: 5'- CCCAGAAGGTGAGAAA -3'

Mice EGFR exon 19 reverse: 5'- TAGTGAGACATAAAAGAAAAC -3'

Mice EGFR exon 20 forward: 5’- ACCAGCCAGGAAACA -3’

Mice EGFR exon 20 reverse: 5’- ACAGACCTCCCAACG -3’

Since that human 21 exon and mouse 21 exon are highly homologous (about 98 %, from NCBI, the human EGFR 21 exon primers were employed for mouse assay.

The electropherograms of exon 19 (Figure c), 20 (Figure d) and 21 (Figure e) demonstrate wild type of EGFR.

Among all 20 single cells, accurate sequences were acquired on 19 cells.

Supplementary Data S7

Considering this assay as a random sampling, we firstly calculated the ideal sample size n_{srs} for a simple random sampling (SRS), then we can calculate the required sample size n_{crs} for a complex random sampling (CRS)[3], which is situation of our assays, as:

$$n_{crs} = n_{srs} \times deff \quad (4)$$

in which $deff$ is the design effect, and

$$n_{srs} = \frac{\mu_{1-\frac{\alpha}{2}}^{2} PQ}{d^2} \quad (5)$$

in which P was set at 30% (0.3), since the average EGFR mutation rate in EGFR expressed cells is 30%[6, 7]; $Q = 1 - P = 0.7$; Confidence interval α was set at 90% (0.9); Error Limits d was set at 10% (0.1); $\mu_{1-\frac{\alpha}{2}}$ was set at 1.645. Therefore,

$$n_{srs} = \frac{\mu_{1-\frac{\alpha}{2}}^{2} PQ}{d^2} = \frac{1.645^2 \times 0.3 \times 0.7}{0.1^2} \approx 57$$

Considering the success rate of our chip is 95%, the n_{srs} was modified to

$$57 \div 95\% = 60$$

The $deff$ was set at 1.5[4]. Finally, the required sample size of our method for each patient n_{crs} was calculated as:

$$n_{crs} = modified\, n_{srs} \times deff = 60 \times 1.5 = 90$$

The sample size 90 is larger than a wildly accepted value for clinical studies, 85[8].

Supplementary Figure S8

Design of a clinical study

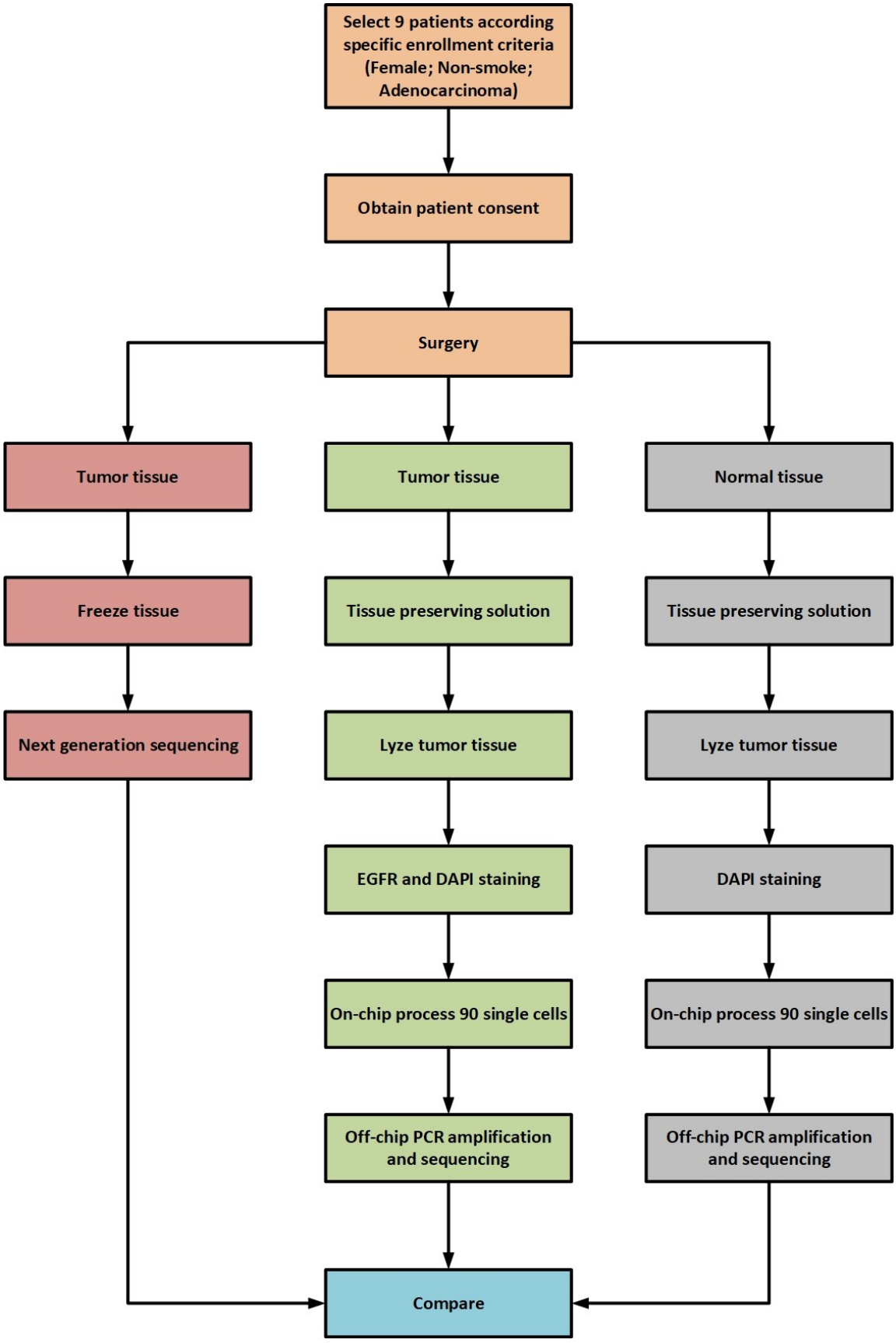

After establishing an enrollment criterion (female, non-smoker, adenocarcinoma) for NSCLC patients who need surgery. 9 patients will be enrolled in this study. Each surgery sample of tumor tissue will be divided into 2 parts, one for our method, the other one for NGS. Meanwhile, the normal tissue from the same surgery will also be processed with our method as control. For each tumor tissue sample, 90 EGFR-expressed cells will be selected and sequenced; for each normal tissue sample, 90 cells will be randomly picked for sequencing. We will compare sequencing results from 3 groups to evaluate the performance of our method on detecting the existence of specific drug-related mutations, EGFR and TP53.

Supplementary Table S9

Cost comparison between NGS and out method

Chip based sequencing cost	
Item	**Cost ($)**
Chip	1/chip (20 cell)
MDA	0.05/cell
PCR	1.2/cell
Sequencing	3/cell
Total	4.3/cell
90 cells cost	**387**

NGS cost	
Item	**Cost ($)**
NGS (Burning Rock)	**2000/Sample**

Price unit is U.S. dollar. The prices for both NGS and Sanger's sequencing were selected from the commercial corporations in Beijing which offered the best price.

References

1. F. B. Dean, S. Hosono, L. Fang, X. Wu, A. F. Faruqi, P. Bray-Ward, Z. Sun, Q. Zong, Y. Du and J. Du, *Proc Natl Acad Sci U S A*, 2002, **99**, 5261-5266.
2. M. Canale, E. Petracci, A. Delmonte, E. Chiadini, C. Dazzi, M. Papi, L. Capelli, C. Casanova, N. De Luigi and M. Mariotti, *CLIN CANCER RES*, 2017, **23**, 2195-2202.
3. J. M. Lachin, *Controlled Clinical Trials*, 1981, **2**, 93-113.
4. E. Vierron and B. Giraudeau, *BMC Med. Res. Method.*, 2009, **9**, 1-9.
5. G. Liu and K. Y. Liang, *Biometrics*, 1997, **53**, 937-947.
6. S. S. Sridhar, L. Seymour and F. A. Shepherd, *Lancet Oncol.*, 2003, **4**, 397-406.
7. H. Bai, Z. Wang, K. Chen, J. Zhao, J. J. Lee, S. Wang, Q. Zhou, M. Zhuo, L. Mao and T. An, *J CLIN ONCOL*, 2012, **30**, 3077.
8. C. Smith, C. Burley, M. Ireson, T. Johnson, D. Jordan, S. Knight, T. Mason, D. Massey, J. Moss and K. Williams, *J. Antimicrob. Chemother.*, 1998, **41**, 467-480.